ISSN 1027-4510, Journal of Surface Investigation: X-ray, Synchrotron and Neutron Techniques, 2020, Vol. 14, Suppl. 1, pp. S169–S174. © Pleiades Publishing, Ltd., 2020.

Neutron Ray-Tracing Simulations of a New Supermirror Guide for the Osiris Spectrometer

A. Perrichon[a, b, *], F. Fernandez-Alonso[b, c], M. Wolff[a], M. Karlsson[d], and F. Demmel[b]

[a] *Department of Physics and Astronomy, Uppsala University, Uppsala, 752 37 Sweden*
[b] *ISIS Facility, Rutherford Appleton Laboratory, Chilton, Didcot, Oxfordshire, OX11 0QX United Kingdom*
[c] *Department of Physics and Astronomy, University College London, London, WC1E 6BT United Kingdom*
[d] *Department of Chemistry and Chemical Engineering, Chalmers University of Technology, Göteborg, 412 96 Sweden*
**e-mail: adrien.perrichon@stfc.ac.uk*

Received June 29, 2019; revised July 31, 2019; accepted August 5, 2019

Abstract—A new supermirror guide has been proposed to replace the current neutron guide of the indirect time-of-flight near-backscattering spectrometer OSIRIS at the ISIS facility. Here we present an extensive Monte Carlo simulation study for the design and optimisation of a new guide system. Among the several guide geometry assessed, a curved guide with elliptical defocusing and focusing sections is shown to perform best. The estimated gain in intensity is a factor of 5–6 at the sample position with a homogeneous distribution of the divergence. The elliptic geometry results in a smaller beam spot and smaller samples will particularly benefit from this upgrade. The proposed guide replacement will ensure that the OSIRIS spectrometer will remain competitive in the years to come.

Keywords: neutron spectrometer, Monte Carlo simulations, OSIRIS, quasielastic neutron scattering
DOI: 10.1134/S1027451020070381

INTRODUCTION

Quasielastic neutron scattering studies are traditionally performed on time-of-flight (TOF) and backscattering spectrometers. At pulsed sources, the idea of backscattering from an analyzer crystal has been combined with the analysis of the incoming energy by measuring the time-of-flight to the detector. One of the first instruments of this type was IRIS at the ISIS Facility (Rutherford Appleton Laboratory, Didcot, UK) [1, 2]. The OSIRIS spectrometer, based on a similar design as IRIS, achieved a large gain in intensity by using a supermirror guide and an analyzer unit with increased angular coverage [3–5]. An extensive Monte Carlo simulation study, using the McStas program package [6–8], was performed to describe in detail the resolution and line shape of the spectrometer [9]. OSIRIS is mainly used as a cold TOF-spectrometer in quasielastic neutron scattering experiments to reveal stochastic particle dynamics and for high-resolution investigations of low-energy excitations (for example, [10, 11]). On the quasielastic side of applications, a strong increase in ion-mobility studies for battery materials has recently been observed. These are quite challenging experiments, since, compared to hydrogen, the studied ions are weak incoherent scatterers [12], which leads to low count-rates of detected neutrons. Here we propose a substantial increase in flux with a new supermirror guide, which will benefit these studies in particular.

The current OSIRIS guide, constructed in the mid-90s, is a $m = 2$ supermirror guide with a $m = 3.6$ straight focusing section at the end of its course, where m stands for an angle of total reflection θ_c of m-times the critical angle of reflection of natural-Ni-coated guides, θ_c^{Ni}. The guide is curved with a radius of curvature of $R = 2050$ m to avoid direct line-of-sight, and has a constant cross section before it converges. The radius of curvature corresponds to a cutoff wavelength of $\lambda_c \approx 2\pi\sqrt{(2a/R)}/(mk_\perp) = 1.90$ Å, with $k_\perp = 0.0107$ Å^{-1} being the perpendicular component of the wavevector for a natural-Ni-coated guide with a width of $a = 43$ mm. At the characteristic wavelength λ_c, the transmission of the curved guide is reduced to 2/3 compared to a straight guide, which indicates a lower limit of useful wavelengths. Incoming energies up to about 20 meV and, hence, energy transfers up to 18 meV can be exploited on OSIRIS (for example, [13, 14]). At the end of the guide, the $m = 3.6$ straight focusing section reduces the beam area from 43 × 65 to 22 × 44 mm. The distance between the guide end and the sample position is 250 mm. At the time of implementation, such a guide was state-of-the-art.

The even older neutron guide of the IRIS spectrometer is a natural-Ni-coated guide ($m = 1$), with a

$m = 2$ focusing section. Interestingly, the measured intensity gain of the OSIRIS guide in comparison to the IRIS guide, at the working wavelength $\lambda = 6.6$ Å, is only about a factor 1.6, which is smaller than expected. Even though the supermirror guide accepts significantly more neutrons, its straight geometry with narrow width and small height leads to a poor transmission due to reflection losses for cold neutrons. This low transmission has been documented through simulations and measurements (for example, [4]). A solution to this challenge is a guide with a different geometry that minimizes the number of reflections. The performance of several guide geometries has been assessed in literature [15–21]. The elliptic geometry emerged as the most favourable one, showing a high transmission of 80% for cold neutrons over distances even longer than the 34 m on OSIRIS [22]. A new guide with an elliptic geometry is therefore proposed to replace the current guide on OSIRIS. Furthermore, the use of elliptic- or parabolic-focusing sections would allow the focusing of the neutrons onto smaller samples.

Since the guide has to replace the existing one, several constraints have to be obeyed, such as the position and angle of the shutter insert by the moderator, and the position of the sample, which makes a curved section necessary and also dictates the length of the guide. In addition, the direct line-of-sight must be avoided, which limits the maximum width of the guide.

SIMULATIONS

The Monte Carlo simulations were performed using the McStas ray-tracing package [6–8], automated with an in-house Matlab code. Specifically, the parameters defining the instrument geometry were calculated with Matlab, then fed to McStas for single-core one-time simulations. Repetitions of the simulations to increase statistics, scans through instrument parameters and analyses of the simulations were controlled and performed in a systematic manner with Matlab.

The first McStas component, ViewModISISver1, characterizes the ISIS source seen through the 25 K hydrogen moderator leading to the OSIRIS and IRIS instruments. For the optimization part of the study, we have considered neutrons with energies of 1.4–4.0 meV, corresponding to a band of wavelengths of about 4.5–7.6 Å, a range used for most experiments on OSIRIS. The guide is modelled with the Guide, Guide_curved, and Elliptic_guide_gravity components for the straight, curved, and elliptically and parabolically tapered defocusing/focusing sections, respectively. For the current OSIRIS guide, the standard reflectivity profile is used[1], with $\alpha = 6.0$ Å being the linear decrease in reflectivity beyond $m = 1$. This figure corresponds to a reflectivity of about 88% at the $m = 2$ edge. For the proposed guide, however, we considered the recent developments in guide fabrication techniques that lead to reflectivities of about 80, 72 and 63% at the $m = 4$, $m = 5$ and $m = 6$ edges [24], respectively, which corresponds to $\alpha \approx 3.5$ Å. We optimized the integrated intensity at the sample position, which was defined as a rectangle of 2 × 3 cm (large sample) and a square of 1 × 1 cm (small sample). The large sample is the standard size for quasielastic neutron scattering experiments, and the smaller sample resembles typical single-crystals or biological samples. The spatial distribution and divergence of the neutron beam at the sample position is monitored by superimposed components, PSD_monitor (two-dimensional (2D)) and PSDlin_monitor (one-dimensional (1D)) for the beam spatial distribution, and Divergence_monitor (2D) and Hdiv_monitor (1D) for the beam divergence.

The current OSIRIS guide was modelled following the description given above, based on technical drawings. Its associated neutron-beam profile in terms of spatial distribution and divergence was used as reference. The proposed elliptically tapered guide is schematically shown in Fig. 1. It consists of three sections: an elliptically shaped defocusing section of length L_{DEF}; a curved guide with constant cross section of length L_{CURVED} and curvature radius R; and an elliptically shaped focusing section of length L_{FOC}. Because of the constraints on the moderator and sample positions, defining the length of two half-ellipses determines the length and curvature radius of the curved section. Vertically, defining the maximum height of the guide (H_{MAX}, in the curved section) and the focal point position of the two half-ellipses determines the height at the guide entrance and exit, H_{IN} and H_{OUT}, respectively. Note that the focal points are defined by their distance from the guide entrance and exit, $L_{DEF.FP,y}$ and $L_{FOC.FP,y}$, respectively. The same applies horizontally, with the width W_{MAX} and focal points $L_{DEF.FP,x}$ and $L_{FOC.FP,x}$ determining the width at the guide entrance W_{IN} and exit W_{OUT}. There is, however, a need to avoid direct line-of-sight (solid line in Fig. 1). For that, we defined the distance at which the line-of-sight is intercepted by the guide wall, L_{LOS}. The intercept condition between the line-of-sight and the curved-guide wall is then evaluated and, if not achieved, the maximum width of the guide is reduced, which redefines the guide entrance and exit widths. This process is repeated till convergence, which leads to the geometry with the maximum guide width that satisfies the aforementioned line-of-sight constraint. Finally, the m-values of the guide are determined by progressively lowering it from $m = 6$ to $m = 4$, in sections from the guide entrance and exit, with each section length to be optimized independently. Note that

[1] See McStas documentation [23] for the empirical formula modelling the reflectivity profile.

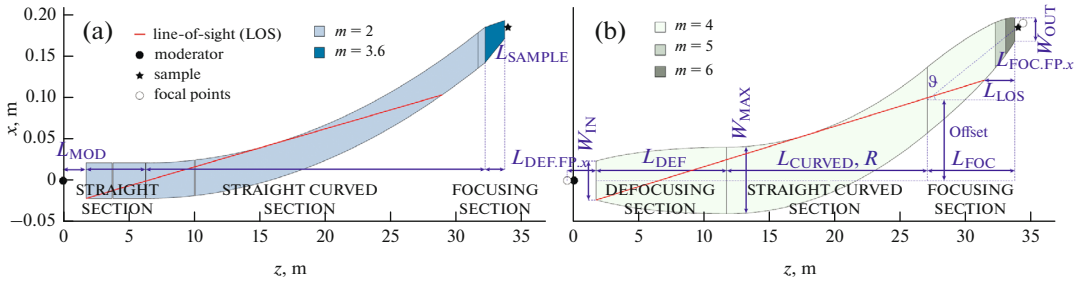

Fig. 1. Scheme (a) of the current OSIRIS guide and (b) optimized elliptically tapered guide, as modelled in McStas and Matlab, from moderator (left) to sample (right). The parameters defining the elliptically tapered guide geometry are indicated: length of the defocusing section (L_{DEF}), length of the curved section (L_{CURVED}), length of the focusing section (L_{FOC}), maximum width of the guide (W_{MAX}), width at guide entrance (W_{IN}), width at guide exit (W_{OUT}), curvature radius (R), distance between the focal point of the defocusing section half-ellipse and the guide entrance ($L_{DEF.FP,x}$), distance between the focal point of the focusing section half-ellipse and the guide exit ($L_{FOC.FP,x}$), distance between the moderator and the guide entrance (L_{MOD}), distance between the guide exit and the sample (L_{SAMPLE}), and distance at which the line-of-sight (LOS) is intercepted from the guide exit (L_{LOS}).

some engineering constraints have been implied, notably concerning the guide height, which is a concern for the size of the shutter insert and the diameter of the bandwidth chopper discs.

We also evaluated alternative geometries, such as guides with parabolic defocusing or focusing sections, and guides with a double ellipse with kink geometry. The same process, as described above, is used for the parabolic tapered guides, with the difference of the focal point definition. Considering the focal point before the defocusing section defined by $L_{DEF.FP}$, the focal point after the section would be at a distance $L_{DEF.FP} + L_{DEF}$ in the elliptic case, and sent to infinity (in practice 10^5 m) in the parabolic case. The same is true for the focusing section. These alternative geometries (some of them reported below) are outperformed by the elliptically tapered guide.

RESULTS AND DISCUSSION

In Table 1, we report the intensity gain factor over the small and large samples, for a set of optimized guide geometries. For all models, the parameter controlling the line-of-sight intercept point (L_{LOS}) is set to 2.2 m, which leads to a similar intercept as for the current OSIRIS guide. The simulations indicate larger gain factors for curved guides with elliptic defocusing and focusing sections (C4). A decrease in the guide height, driven by engineering constraints, reduces the gain factor over the large sample. This effect can be partially overcome by increasing the curvature of the guide (smaller radius R), which increases the maximum guide width but leads to an increase in the minimum m-value from 3 to 4. Note that increasing the minimum m-value of the guide to $m = 4$ is beneficial for the transport of short-wavelength neutrons. The

Table 1. Gain factor for small (1 × 1 cm) and large (2 × 3 cm) samples, as defined in the main text, and for a set of optimized guide geometries (constraints are applied on the maximum height of the guide (H_{MAX}) and the curvature radius (R))

Label	Geometry	Constraints	Gain 1 × 1	Gain 2 × 3
A	OSIRIS guide (reference)	–	1	1
B	Double ellipse with a kink	$H_{MAX} \le 25$ cm	4.7	4.7
C1	Curved, parabolic defocusing/focusing	$R \ge 1.5$ km, $H_{MAX} \le 25$ cm	3.5	3.4
C2	Curved, elliptic defocusing, parabolic focusing	$R \ge 1.5$ km, $H_{MAX} \le 25$ cm	4.2	4.3
C3	Curved, parabolic defocusing, elliptic focusing	$R \ge 1.5$ km, $H_{MAX} \le 25$ cm	4.6	4.4
C4a	Curved, elliptic defocusing/focusing	$R \ge 1.5$ km, $H_{MAX} \le 25$ cm	5.9	5.6
C4b	Curved, elliptic defocusing/focusing	$R \ge 1.5$ km, $H_{MAX} \le 20$ cm	5.7	5.0
C4c	Curved, elliptic defocusing/focusing	$R \ge 1.2$ km, $H_{MAX} \le 20$ cm	5.9	5.2

Table 2. Parameters associated to the optimized elliptically tapered guide (C4c, Fig. 1)

Parameter	Value	Parameter	Value
$L_{DEFOCUSING}(*)$	10.00	$H_{MAX}(*)$	0.200
$L_{FOCUSING}(*)$	6.70	H_{IN}	0.090
L_{CURVED}	15.35	H_{OUT}	0.050
Radius, R	1208	W_{MAX}	0.081
Offset	0.10	W_{IN}	0.047
θ, deg	0.728	W_{OUT}	0.028
$L_{DEF.FP.x}(*)$	2.30	$L_{FOC.FP.x}(*)$	0.45
$L_{DEF.FP.y}(*)$	1.20	$L_{FOC.FP.y}(*)$	0.22
$L_{FOC.m=5}(*)$	0.80	$L_{FOC.m=6}(*)$	0.70

Parameters marked with (*) are optimized and determine the remaining parameters. If not specified otherwise, parameter values are in meters. The line-of-sight intercept point (L_{LOS}) is set at 2.2 m from the guide exit.

best-performing design for the given constraints (C4c) is associated to gain factors of 5.9 and 5.2, for the small and large samples, respectively. The guide is represented in Fig. 1, and its geometric parameters are summarized in Table 2. Given the optimized curvature radius of R = 1208 m, the guide width of 81 mm and the m = 4 coating, the cutoff wavelength is $\lambda_c \approx 1.70$ Å, comparable to the value of 1.90 Å of the current guide.

Figure 2 shows the spatial distribution and divergence of the neutron beam at the sample position for the current OSIRIS guide and for the optimized elliptically tapered guide (C4c). The OSIRIS guide is characterized by an oblong spatial distribution of dimensions 20 × 40 mm (FWHM) and a peaked divergence of about 3° horizontally and vertically. The optimized elliptically tapered guide shows a more focused beam of dimensions 20 × 30 mm and more homogeneous and broader divergence of about 4° horizontally and 8° vertically. The smaller beam size of the new design will allow routine measurements of much-smaller samples. The increase in divergence can be detrimental for some studies, in particular when momentum resolution is required, for example, for diffraction and low-energy dispersive excitations in single crystals. A set of movable slits will be inserted into the focusing section to adjust the divergence, if required. Such an approach has been successfully used in the WISH diffractometer at the ISIS Facility [25].

Figure 3 shows the intensity and gain factors of the optimized guide as a function of neutron wavelength. The maximum gain is found at $\lambda \approx 4.0$ Å with a factor of 7.4 and 6.1 for the small and large samples, respectively. In the wavelength range most often used on OSIRIS, between $\lambda = 4.0$ and 7.0 Å, the gain factor is around 5 or larger. The decrease in the gain factor at the edges of the wavelength band is expected, since the optimization was done for energies of E_i = 1.4–4.0 meV. The simulations done in this work do not take into account that the actual OSIRIS guide has aged over the past 20 yrs. Estimates at other facilities suppose a 50% loss in guide transmission for cold neutrons over such a time span. Thus, an increase in

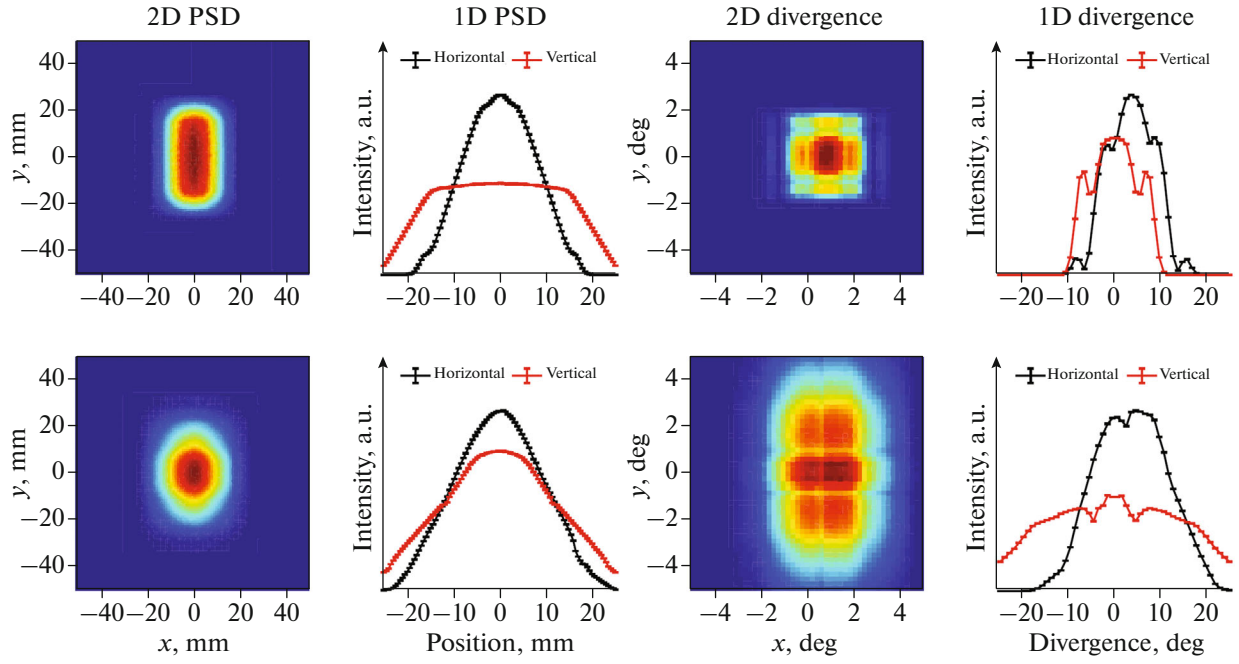

Fig. 2. Comparison of the spatial distribution (2D and 1D PSD) and divergence (2D and 1D) of the neutron beam at the sample position for (top) the current OSIRIS guide and (bottom) the optimized elliptically tapered guide (C4c).

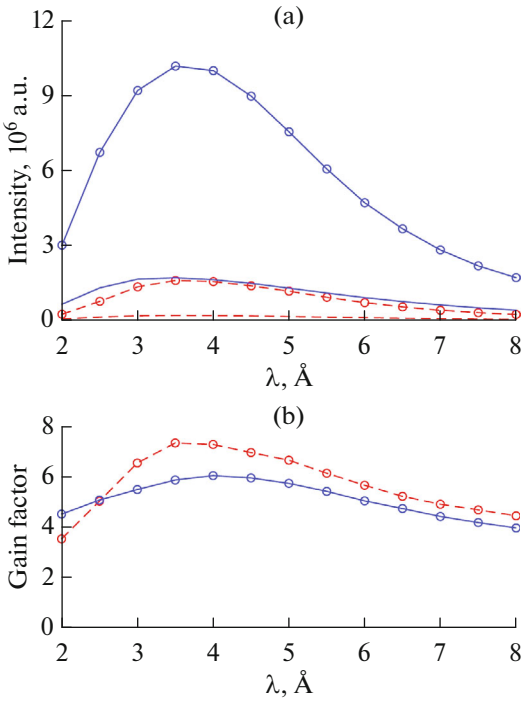

Fig. 3. (a) Intensity and (b) gain factor of the elliptically tapered guide (C4c, lines with circles) as a function of neutron wavelength, λ, for small (1 × 1 cm) (red dashed line) and large (2 × 3 cm) (blue solid line) samples. Each point corresponds to a range of wavelength of 0.5 Å centred at the selected λ. The performance of the current OSIRIS guide is indicated as well (lines without markers).

intensity of an order of magnitude can be expected with the elliptically tapered guide, compared to the current instrument, which would be transformative for many challenging experiments.

CONCLUSIONS

Detailed Monte Carlo simulations have been performed to assess the performance of a new high-*m* supermirror guide for the OSIRIS spectrometer. The best design is a curved guide with elliptically shaped defocusing and focusing sections, resulting in an intensity gain of 5–6 at the sample position, and possibly up to an order of magnitude when considering the degradation of the current OSIRIS guide. With this guide upgrade, the OSIRIS spectrometer will be competitive with the other cold neutron time-of-flight spectrometers even at more brilliant sources. This necessary upgrade will ensure a bright future for the instrument and the user community it serves, up to and beyond 2030.

FUNDING

This work was supported by the Science and Technology Facilities Council (STFC) and by the Swedish Research Council (VR, Grant no. 2016-06958).

REFERENCES

1. C. J. Carlile and M. A. Adams, Phys. B (Amsterdam, Neth.) **182,** 431 (1992). https://doi.org/10.1016/0921-4526(92)90047-V
2. C. J. Carlile, M. A. Adams, P. S. R. Krishna, M. Prager, K. Shibata, and P. Westerhuijs, Nucl. Instrum. Methods Phys. Res., Sect. A **338**, 78 (1994). https://doi.org/10.1016/0168-9002(94)90165-1
3. D. Martín y Marero, S. Campbell, and C. J. Carlile, J. Phys. Soc. Jpn. **65**, 245 (1996).
4. M. T. F. Telling, S. I. Campbell, D. Engberg, D. Martín y Marero, and K. H. Andersen, Phys. Chem. Chem. Phys. **7**, 1255 (2005). https://doi.org/10.1039/B413934H
5. F. Demmel, D. McPhail, J. Crawford, D. Maxwell, K. Pokhilchuk, V. Garcia-Sakai, S. Mukhopadyay, M. T. F. Telling, F. J. Bermejo, N. T. Skipper, and F. Fernandez-Alonso, EPJ Web Conf. **83**, 03003 (2015). https://doi.org/10.1051/epjconf/20158303003
6. P. Willendrup, E. Farhi, E. Knudsen, U. Filges, and K. Lefmann, J. Neutron Res. **17**, 35 (2014). https://doi.org/10.3233/JNR-130004
7. P. Willendrup, E. Farhi, and K. Lefmann, Phys. B (Amsterdam, Neth.) **350**, E735 (2004). https://doi.org/10.1016/j.physb.2004.03.193
8. K. Lefmann and K. Nielsen, Neutron News **10** (3), 20 (1999). https://doi.org/10.1080/10448639908233684
9. F. Demmel and K. Pokhilchuk, Nucl. Instrum. Methods Phys. Res., Sect. A **767**, 426 (2014). https://doi.org/10.1016/j.nima.2014.09.019
10. C. Stock, C. Broholm, Y. Zhao, F. Demmel, H. J. Kang, K. C. Rule, and C. Petrovic, Phys. Rev. Lett. **109**, 167207 (2012). https://doi.org/10.1103/PhysRevLett.109.167207
11. W. J. Gannon, I. A. Zaliznyak, L. S. Wu, A. E. Feiguin, A. M. Tsvelik, F. Demmel, Y. Qiu, J. R. D. Copley, M. S. Kim, and M. C. Aronson, Nat. Commun. **10**, 1123 (2019). https://doi.org/10.1038/s41467-019-08715-y
12. T. J. Willis, D. G. Porter, D. J. Voneshen, S. Uthayakumar, F. Demmel, M. J. Gutmann, M. Roger, K. Refson, and J. P. Goff, Sci. Rep. **8**, 3210 (2018). https://doi.org/10.1038/s41598-018-21354-5
13. A. Lovell, F. Fernandez-Alonso, N. T. Skipper, K. Refson, S. M. Bennington, and S. F. Parker, Phys. Rev. Lett. **101**, 126101 (2008). https://doi.org/10.1103/PhysRevLett.101.126101
14. F. Fernandez-Alonso, F. J. Bermejo, C. Cabrillo, R. O. Loutfy, V. Leon, and M. L. Saboungi, Phys. Rev. Lett. **98**, 215503 (2007). https://doi.org/10.1103/PhysRevLett.98.215503
15. C. Schanzer, P. Böni, U. Filges, and T. Hils, Nucl. Instrum. Methods Phys. Res., Sect. A **529**, 63 (2004). https://doi.org/10.1016/j.nima.2004.04.178
16. P. Böni, Nucl. Instrum. Methods Phys. Res., Sect. A **586**, 1 (2008). https://doi.org/10.1016/j.nima.2007.11.059
17. M. Janoschek, P. Böni, and M. Braden, Nucl. Instrum. Methods Phys. Res., Sect. A **613**, 119 (2010). https://doi.org/10.1016/j.nima.2009.10.164

18. C. Pelley, F. Kargl, V. Garcia Sakai, M. T. F. Telling, F. Fernandez-Alonso, and F. Demmel, J. Phys.: Conf. Ser. **251**, 012063 (2010). https://doi.org/10.1088/1742-6596/251/1/012063

19. H. Jacobsen, K. Lieutenant, C. Zendler, and K. Lefmann, Nucl. Instrum. Methods Phys. Res., Sect. A **717**, 696 (2013). https://doi.org/10.1016/j.nima.2013.03.048

20. C. Zendler, D. Nekrassov, and K. Lieutenant, Nucl. Instrum. Methods Phys. Res., Sect. A **746**, 39 (2014). https://doi.org/10.1016/j.nima.2014.01.044

21. D. M. Rodriguez, D. D. DiJulio, and P. M. Bentley, Nucl. Instrum. Methods Phys. Res., Sect. A **808**, 101 (2016). https://doi.org/10.1016/j.nima.2015.11.057

22. K. H. Klenø, K. Lieutenant, K. H. Andersen, and K. Lefmann, Nucl. Instrum. Methods Phys. Res., Sect. A **696**, 75 (2012). https://doi.org/10.1016/j.nima.2012.08.027

23. McStas. http://www.mcstas.org. Accessed June 27, 2019

24. Swiss Neutronics. https://www.swissneutronics.ch. Accessed June 6, 2019

25. L. Chapon, P. Manuel, P. Radaelli, C. Benson, L. Perrott, S. Ansell, N. Rhodes, D. Raspino, D. Duxbury, E. Spill, and J. Norris, Neutron News **22** (2), 22 (2011). https://doi.org/10.1080/10448632.2011.569650